Supplementary Information

Tuning Co/Ni ratio in Co-Ni bimetallic hybrid for electrochemical detection of glucose

Junyi Zeng[1], Yanting Yang[2], Xiaoyu Lei [1], Jinan Deng[1]*, Ning Hu[1]* and Jun Yang[1]*

[1] Key Laboratory of Biorheological Science and Technology, Ministry of Education and Bioengineering College, Chongqing University, Chongqing 400044, China

[2] College of Animal Science and Technology, Southwest University, Chongqing 402460, China.

*Corresponding authors:

biojdeng@cqu.edu.cn (J. Deng)

huning@cqu.edu.cn (N.Hu)

bioyangjun@cqu.edu.cn (J. Yang)

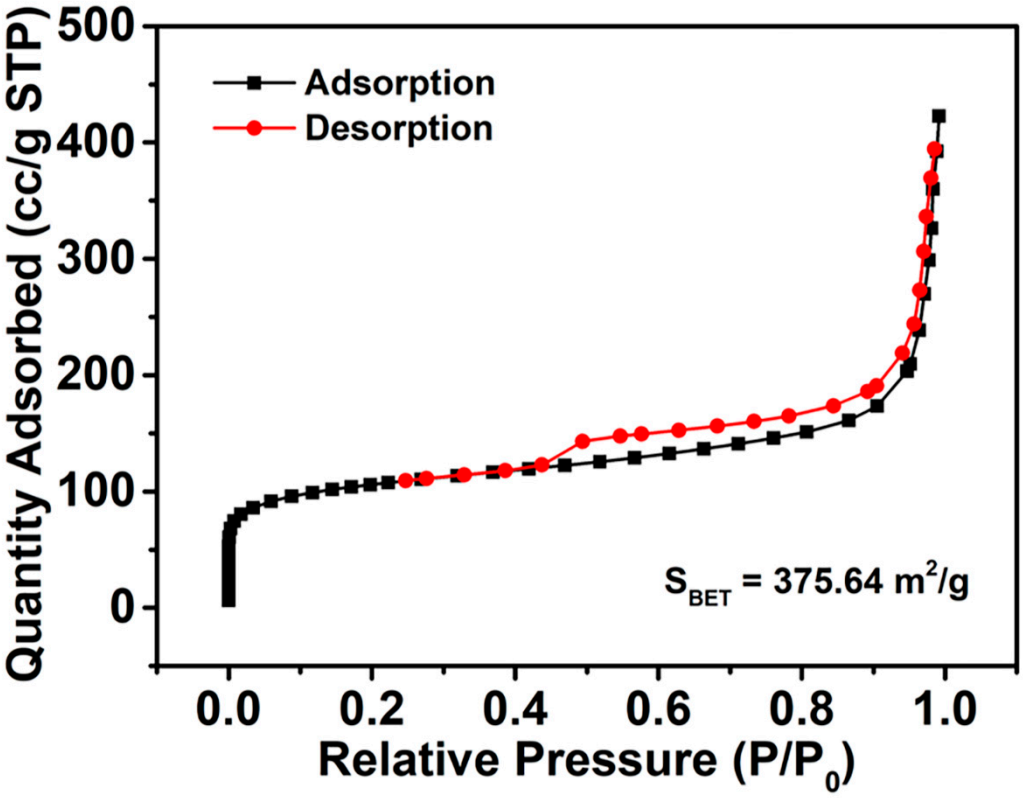

Figure S1. N_2 adsorption/desorption isotherm of Co_1Ni_1/N-C hybrid.

Table S1 Specific surface areas of hybrids calculated by BET method

Hybrid	S_{BET} (m^2/g)
Co/N-C	233.45
Co_3Ni_1/N-C	235.45
Co_1Ni_1/N-C	375.64
Co_1Ni_3/N-C	309.37
Ni/N-C	314.64

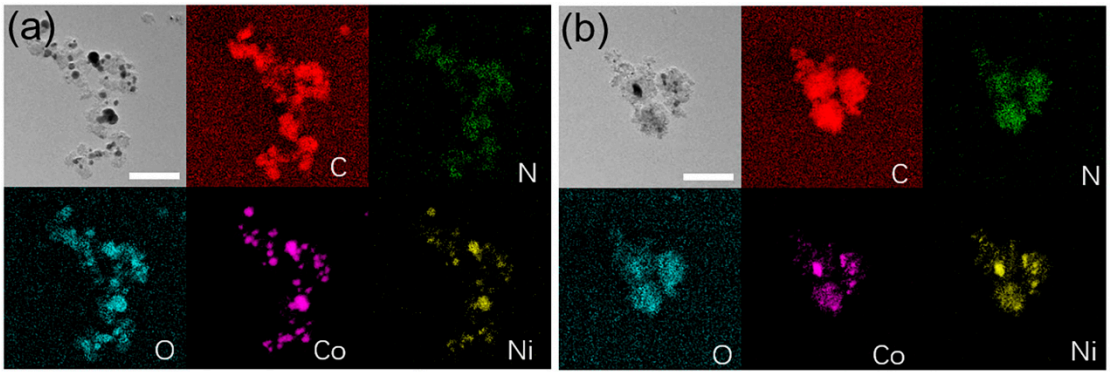

Figure S2. The TEM images and the corresponding elemental mapping images of (a) Co_3Ni_1/N-C and (b) Co_1Ni_3/N-C hybrids for C, N, O, Co, and Ni. The scale bar is 500 nm

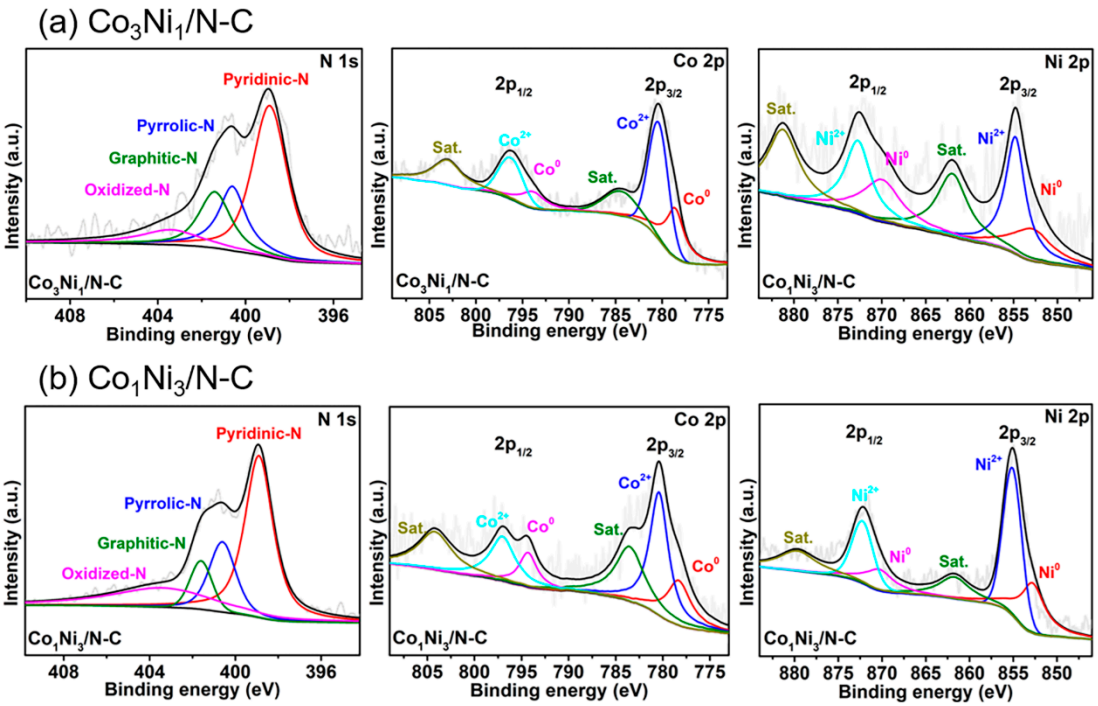

Figure S3. XPS spectra of C 1s, N 1s, Co 2p, and Ni 2p for (a) Co_3Ni_1/N-C and (b) Co_1Ni_3/N-C hybrids

Table S2. N contents calculated from XPS spectra

Hybrid	Pyridinic N (%)	Pyrrolic N (%)	Graphitic N (%)	Oxidized N (%)
Co/N-C	49.0	19.3	19.6	12.1
Co_3Ni_1/N-C	51.2	20.2	18.8	9.8
Co_1Ni_1/N-C	50.8	21.3	15.4	12.5
Co_1Ni_3/N-C	51.0	19.1	10.0	19.9
Ni/N-C	42.5	27.0	19.4	11.1

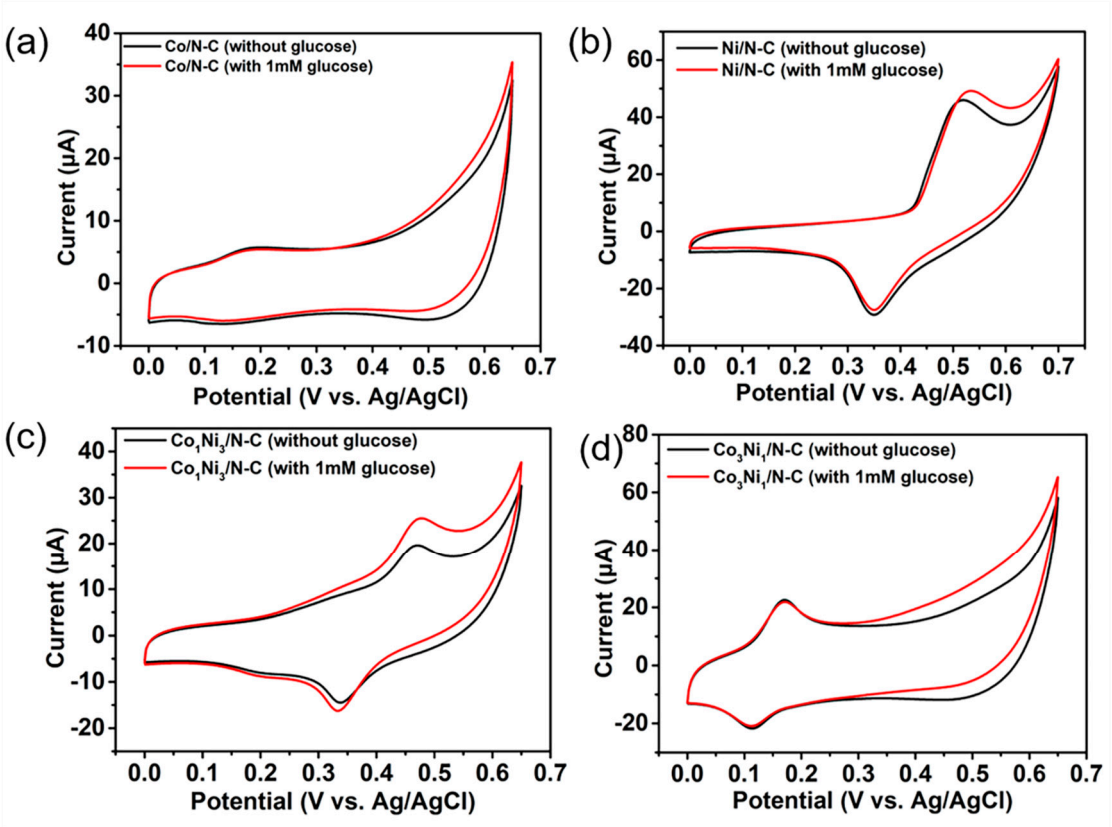

Figure S4. CV curves of SPEs modified with (a) Co/N-C, (b) Ni/N-C, (c) Co_1Ni_3/N-C, and (d) Co_3Ni_1/N-C hybrids in 0.1 M NaOH aqueous solution in the absence and presence of 1 mM glucose at a scan rate of 50 $mV \cdot s^{-1}$.

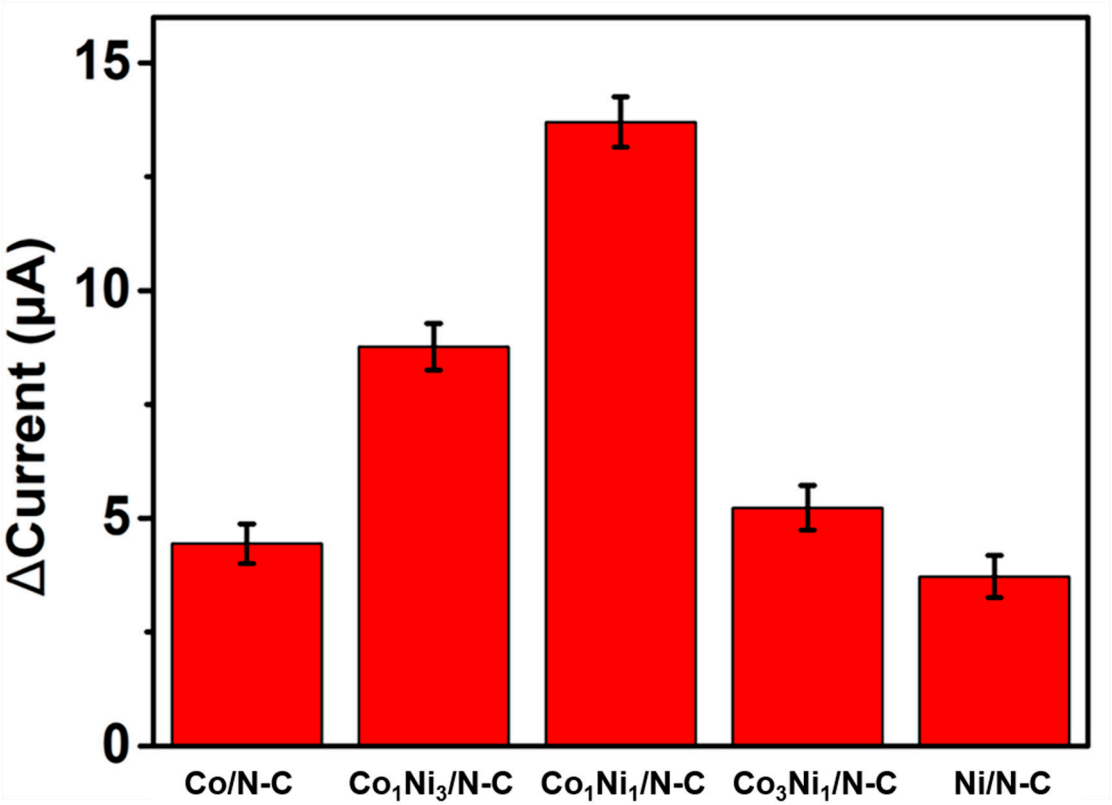

Figure S5. The current increment extracted from the CVs of hybrid-modified SPEs with different Co/Ni ratios at 0.6 V in presence of 1 mM glucose at a scan rate of 50 $mV \cdot s^{-1}$.

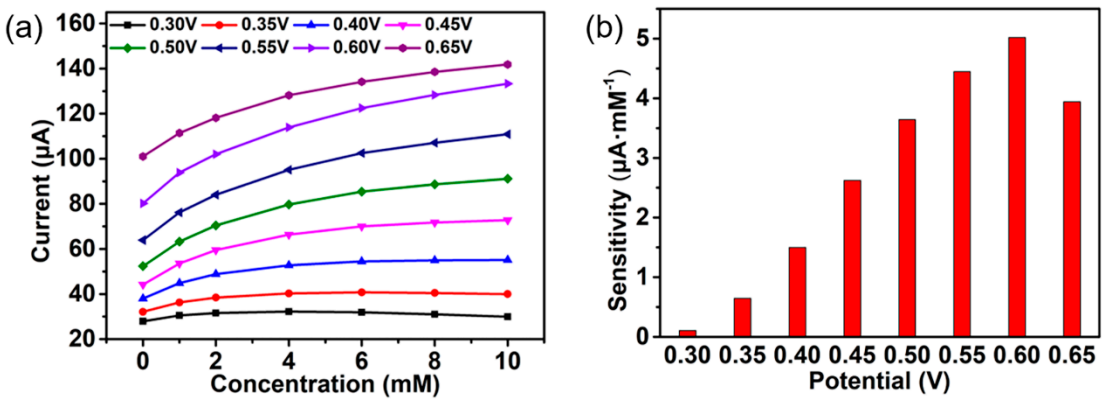

Figure S6. Current response of CO_1Ni_1/N-C-modified SPE as a function of glucose concentration in 0.1 NaOH aqueous solution at various applied potentials (a) and the corresponding sensitivity at different applied potentials (b).

Table S3 Comparison of the sensing performance of Co_1Ni_1/N-C hybrid-modified SPE prepared in this work with other non-enzymatic glucose sensors

Electrode	Sensitivity ($\mu A \cdot mM^{-1} \cdot cm^{-2}$)	Electrolyte	Linear range	LOD (μM)	Ref.
$NiCo_2O_4$/N-rGO	3210	0.1 M KOH	15 μM–2.55 mM	0.18	[1]
NiCo/C	265	0.1 M NaOH	0.5 μM–4.38 mM	0.2	[2]
NiO-$NiCo_2O_4$/C	340.4 56.1	0.1 M NaOH	0.1 μM–600 μM 0.9–6.3 mM	0.03	[3]
$NiCo_2O_4$ nanosphere	1917 703	0.2 M NaOH	0.01–0.30 mM, 0.3–2.24 mM	0.6	[4]
$NiCo_2O_4$ nanorods	1685	0.1 M NaOH	0.1 μM–1.0 mM	0.16	[5]
Ni/Co(HHTP)MOF/CC	3250	0.1 M NaOH	0.3 μM–2.312 mM	0.1	[6]
NiCo LDH	30.59	0.1 M NaOH	5–25 mM	530	[7]
Ni-Co MOF/Ag/rGO/PU	425.9	0.1 M NaOH	10 μM–0.66mM	3.28	[8]
NiCo-LDH	4600	0.1 M NaOH	Up to 2.5 mM	0.2	[9]
NiCo-MOF nanosheets	684.4	0.1 M NaOH	1 μM–8 mM	0.29	[10]
Co_1Ni_1/N-C	1041.7 75.7	0.1 M NaOH	0.5 μM–1 mM 1–10 mM	0.11	This work

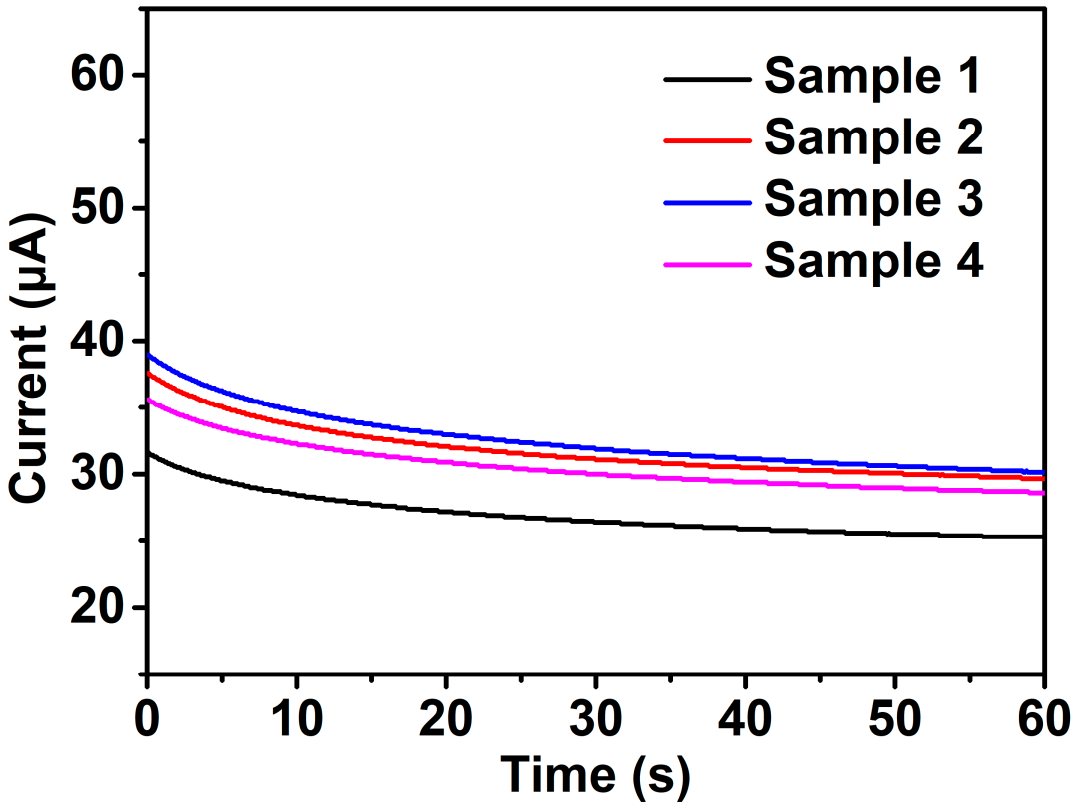

Figure S7. Amperometric response of CO_1Ni_1/N-C hybrid-modified SPE for glucose determination using serum samples.

References

1. Sheng, Q.; Liu, D.; Zheng, J. Nico alloy nanoparticles anchored on polypyrrole/reduced graphene oxide nanocomposites for nonenzymatic glucose sensing. *New J. Chem.* **2016**, *40*, 6658-6665. https://doi.org/10.1039/c6nj01264g
2. Wang, L.; Hou, C.; Yu, H.; Zhang, Q.; Li, Y.; Wang, H. Metal–organic framework-derived nickel/cobalt-based nanohybrids for sensing non-enzymatic glucose. *ChemElectroChem* **2020**, *7*, 4446-4452. https://doi.org/10.1002/celc.202001135
3. Wang, L.; Yu, H.; Zhang, Q.; Li, Y.; Jia, W.; Hou, C.; Wang, H. Nico–nicoo2/carbon hollow nanocages for non-enzyme glucose detection. *Electrochim. Acta* **2021**, 381, 138259. https://doi.org/10.1016/j.electacta.2021.138259
4. Huang, W.; Cao, Y.; Chen, Y.; Peng, J.; Lai, X.; Tu, J. Fast synthesis of porous nico2o4 hollow nanospheres for a high-sensitivity non-enzymatic glucose sensor. *Appl. Surf. Sci.* **2017**, *396*, 804-811. https://doi.org/10.1016/j.apsusc.2016.11.034
5. Yang, J.; Cho, M.; Lee, Y. Synthesis of hierarchical nico2o4 hollow nanorods via sacrificial-template accelerate hydrolysis for electrochemical glucose oxidation. *Biosens. Bioelectron.* **2016**, *75*, 15-22. https://doi.org/10.1016/j.bios.2015.08.008
6. Xu, Z.; Wang, Q.; Zhangsun, H.; Zhao, S.; Zhao, Y.; Wang, L. Carbon cloth-supported nanorod-like conductive ni/co bimetal mof: A stable and high-performance enzyme-free electrochemical sensor for determination of glucose in serum and beverage. *Food Chem.* **2021**, *349*, 129202. https://doi.org/10.1016/j.foodchem.2021.129202
7. Wu, Y. T.; Tsao, P. K.; Chen, K. J.; Lin, Y. C.; Aulia, S.; Chang, L. Y.; Ho, K. C.; Chang, C.Y.; Mizuguchi, H.; Yeh, M. H. Designing bimetallic ni-based layered double hydroxides for enzyme-free electrochemical lactate biosensors. *Sens. Actuators B Chem.* **2021**, *346*, 130505. https://doi.org/10.1016/j.snb.2021.130505
8. Shu, Y.; Su, T.; Lu, Q.; Shang, Z.; Xu, Q.; Hu, X. Highly stretchable wearable electrochemical sensor based on ni-co mof nanosheet-decorated ag/rgo/pu fiber for continuous sweat glucose detection. *Anal. Chem.* **2021**, *93*, 16222-16230. https://doi.org/10.1021/acs.analchem.1c04106
9. Amin, K.M.; Muench, F.; Kunz, U.; Ensinger, W. 3d nico-layered double hydroxide@ni nanotube networks as integrated free-standing electrodes for nonenzymatic glucose sensing. *J. Colloid Interface Sci.* **2021**, *591*, 384-395. https://doi.org/10.1016/j.jcis.2021.02.023
10. Li, W.; Lv, S.; Wang, Y.; Zhang, L.; Cui, X. Nanoporous gold induced vertically standing 2d nico bimetal-organic framework nanosheets for non-enzymatic glucose biosensing. *Sens. Actuators B Chem.* **2019**, *281*, 652-658. https://doi.org/10.1016/j.snb.2018.10.150